ESA/ESOC Contract No. 13037/98/D/IM

Study Note of Work Package 1

Model for the Initial Population

Prepared by

Carmen Pardini

Revised and Approved by

Luciano Anselmo

17 January 2000

Consorzio Pisa Ricerche

TABLE OF CONTENTS

INTRODUCTION

Beside 8000-9000 objects larger than 10-20 cm tracked by the US Space Command sensors, the circumterrestrial space is populated by a very large number of artificial debris, down to sub-millimeter particles, produced over the years and continually replenished by international space activities. Particles in the millimeter and centimeter size range are particularly interesting because they can seriously damage critical spacecraft sub-systems.

Most of the experimental data available in this debris size range comes from dedicated campaigns of radar measurements carried out since 1990 by several facilities in the United States and Europe. The main outcome of such data was to show the very large number of millimeter and centimeter particles present in space, much more than expected.

Environmental models were developed following, basically, two approaches. In one of them, environmental debris models were developed emphasizing the consistency with measurements in low earth orbit, more than the detailed description of the source mechanisms and mechanics. Such *engineering models*, like NASA's ORDEM96 (Kessler et al., 1996) are useful operational tools to predict debris fluxes on low earth satellites, in agreement with the available database and the models used to fit the measurements. The *evolutionary models*, like the ESA's MASTER (Sdunnus, 1995), consisted instead in identifying the candidate source and sink mechanisms, modeling in detail each single event able to produce debris and propagating the full population of orbital particles to a given reference epoch.

In order to provide initial environment conditions to the Semi-Deterministic Model (SDM) for Space Debris Long-Term Evolution Modeling (Anselmo et al., 1996), an evolutionary model (CODRM-94) was developed at CNUCE in 1994 (Pardini et al., 1995). In September 1997, an improved debris environment model, the 1997.0 CNUCE Orbital Debris Reference Model (CODRM-97), including the RORSAT sodium-potassium droplets, was completed (Pardini et al., 1998).

Recently, a similar work has been repeated to obtain updated environmental initial conditions for the new SDM software, whose extension was carried out in the present contract. The resulting CODRM-99 debris population is the product of a massive effort to estimate the contribution of the historical events in orbit able to produce a large number of particles. The sources considered as of January 1, 1999 - reference epoch of the model - were 154 spacecraft and upper stages breakups and 16 NaK liquid metal leaks from the primary nuclear reactor coolant system of the last Soviet radar ocean reconnaissance satellites (RORSATs).

Over the years, a dedicated software system, CLDSIM (Pardini, 1995) was developed, implemented and continually upgraded and improved to simulate the generation and orbital propagation of debris clouds produced by explosions, collisions and RORSAT-like coolant leakage using several model and parameter options. In particular, it includes one breakup model for low intensity explosions, four models for high intensity explosions, two models for collisions and one model for RORSAT-like events. The largest objects (as defined by the user) and a sample of the smallest ones are propagated using an accurate fast orbit propagator (including all the relevant perturbations), or a much faster debris cloud propagator (including only air drag, varying according to the 11-yr solar activity cycle).

Using CLDSIM, each debris generating event was simulated independently with the most appropriate models and parameters, and the resulting debris clouds were propagated - including all the relevant perturbations - to the chosen reference epoch: January 1, 1999, 00:00 UTC. At this point, the particles obtained were merged with the US Space Command catalogued objects, propagated to the same epoch. The resulting model, CODRM-99, included all the simulated particles larger than 1 mm still in earth orbit at the reference epoch.

In total, more than 21 millions of particles larger than 1 mm resulted still in orbit at the reference epoch. The number of objects actually propagated was close to 186,000, with sampling factors ranging from 1/1000 for the smallest particles (mass lower than 10 mg) to 1/5 (in the 1-100 g range). The objects heavier than 100 g were propagated one by one.

FRAGMENTATION MODELS

CLDSIM simulates a breakup/leakage event by a random extraction of fragments mass/diameter from a given distribution (Pardini, 1995). To generate CODRM-99, only a subset of the fragmentation models built in CLDSIM was used. The models selected are presented in the following sections.

Low Intensity Explosions

To represent the fragment mass distribution for low intensity explosions, the following relationship was adopted (Su and Kessler, 1985):

$$N(m) = \begin{cases} 0.171 M_t e^{-0.6502\sqrt{m}} & m \geq 1.936 \\ 0.869 M_t e^{-1.8202\sqrt{m}} & m < 1.936 \end{cases} \quad (1)$$

where M_t is the exploding mass and N is the cumulative number of fragments with mass larger than m. M_t and m are in kg.

High Intensity Explosions

For high intensity explosions, two mass distribution models were used. Both assume that the 90% of the exploding mass M_t follows an exponential distribution law, while the 10% follow a power law. The requirements of mass conservation and function continuity set the value of the numerical coefficients. One of the models is (Reynolds, 1991):

$$N(m) = \begin{cases} 9.4561 \cdot 10^{-3} M_t / m & m < 0.015 \\ 0.7901 M_t e^{-1.8202\sqrt{m}} & 0.015 \leq m < 1.936 \\ 0.1555 M_t e^{-0.6502\sqrt{m}} & m \geq 1.936 \end{cases} \quad (2)$$

where M_t and m are in kg. The other one was proposed in 1995 by R. Jehn and T. Parrinello of ESA/ESOC (the masses are expressed in kg):

$$N(m) = \begin{cases} N_0 e^{-c\sqrt{m}} & m \geq 0.05 \\ 0.439\left(\dfrac{m}{0.1 \cdot M_t}\right)^{-0.75} & m < 0.05 \end{cases} \quad (3)$$

N_0 and c are calculated such that mass conservation is granted and the function $N(m)$ is continuous.

Collisions

The fragment mass distribution adopted by Reynolds (1991) has been used for collision modeling:

$$N(m) = 0.4396\left(\frac{M_e}{m}\right)^{0.7496} \quad (4)$$

The total mass of the ejecta M_e is given by $1.15v^2m_p$ – where v is the relative impact velocity in km/s and m_p is the projectile mass – if the ratio $(1.15v^2m_p)/M_t < 0.1$ (craterization regime, with $M_t \equiv$ target mass). Otherwise, a catastrophic breakup occurs and $M_e = M_t + m_p$.

RORSAT Liquid Metal Leakage

A few years ago the Haystack and Goldstone radar observations led to the detection of a previously unrecognized space debris family, with circular orbits between 600 and 1000 km of altitude (maximum concentration between 850 and 1000 km) and inclinations around 65° (Stansbery et al., 1996; Stansbery and Settecerri,1997). There were 50,000-70,000 such particles larger than 8 mm and very few were larger than 3 cm. The radar signatures of these objects were characteristic of conductive spheres at every measured wavelength and their ballistic coefficients were consistent with mass densities around 1 g/cm^3.

Due to their orbital and physical properties, these particles were tentatively identified by NASA's Johnson Space Center as droplets of liquid sodium-potassium (NaK) coolant leaked from one or more of the nuclear powered radar ocean reconnaissance satellites (RORSATs) launched by the former Soviet Union. This conclusion was later confirmed by new radar observations (Goldstein et al., 1998) and theoretical analysis.

The origin of this unusual source of space debris can be traced back to the *Cosmos 954* malfunction that led, on January 1978, to the light radioactive contamination of a sparsely inhabited area of northern Canada. To prevent the further occurrence of a similar mishap, the Soviets redesigned the RORSATs, developing a way to eject the fuel core from the reactor at the end of the mission, to ensure the complete burning of the naked fuel core during an accidental reentry in the earth atmosphere.

However, the design change affected also the nominal missions (16 up to the program termination in 1988). The fuel core separation in the graveyard orbit was, in fact, accompanied by a loss of sealing in the primary reactor coolant loop, containing 13 kg of liquid NaK. Therefore, a leakage of NaK droplets occurred. The secondary reactor coolant loop, with 26 kg of liquid NaK, was designed to maintain, instead, its sealing.

By fitting, with the least square method, the size distribution curve observed by the Haystack radar (Stansbery et al., 1996) – for droplets in the 0.5-4.7 cm range – and assuming that the 16 leakage events were comparable, the following size distribution, applicable to each single case, was obtained:

$$N(d) = 4.881 \cdot 10^{-3} d^{-2.6277} \qquad 1.0 \cdot 10^{-3} \leq d \leq 4.7 \cdot 10^{-2} \tag{5}$$

where $N(d)$ is the cumulative number of droplets with a diameter larger than d (meters). The particle mass was computed assuming a spherical shape and a sodium-potassium density of 0.9 g/cm^3.

Particles with $d \geq 1$ mm where considered in the 16 cloud simulations carried out to build the CODRM-99 model. A sodium-potassium leakage according to Eq. (5) was simulated for each of the RORSATs left in orbit between *Cosmos 1176* (launched in 1980) and *Cosmos 1932* (launched in 1988). The events were assumed to occur immediately after the nuclear core ejection in graveyard orbit and every cloud of NaK droplets was propagated to the CODRM-99 reference epoch.

Table 1

RORSAT'S DROPLETS GENERATED AND STILL IN ORBIT AT THE REFERENCE EPOCH (1 JANUARY 1999)

Particle Diameter ≥	Sodium-Potassium Droplets Generated	Particles still in Orbit at the Reference Epoch
1 mm	5,967,224	2,765,569
2 mm	964,224	599,569
3 mm	332,224	244,069
4 mm	156,224	127,969
5 mm	86,944	76,869
6 mm	53,824	49,969
7 mm	35,904	34,314
8 mm	25,264	24,539
9 mm	18,512	18,086
1 cm	13,664	13,414
2 cm	2,064	2,061
3 cm	672	672
4 cm	96	96

The cumulative number of sodium-potassium droplets generated by the model, and still in orbit at the reference epoch, is given in Table 1, as a function of their diameter.

Other European models, like the Meteoroid and Space Debris Terrestrial Environment Reference Model – MASTER- (Klinkrad et al., 1997) and the Integrated Debris Evolution Suite Model – IDES – (Walker et al., 1996), were developed by identifying the candidate source and sink mechanisms, then modeling in detail each single event able to produce debris, and finally propagating the full population of orbital particles to a given reference epoch. These models also include a description of the RORSAT liquid metal leakage, resulting from totally independent and different approaches. Table 2 lists the cumulative number of NaK droplets still in orbit at the reference epoch of the CODRM-99 (January 1, 1999), MASTER-99 (August 1, 1999) and IDES-98 (March 31, 1998) models, as a function of their diameter. The MASTER-99 and IDES-98 data were kindly provided by Peter Wegener (e-mail of December 7, 1999) and Roger Walker (e-mail of December 20, 1999), respectively. In Table 2, data coming from radar observations were presented too. Above 6 mm, these data were derived from the Haystack radar observations (Stansbery and Settecerri, 1997), while below 6 mm they were based on the Goldstone radar outcomes (Goldstein et al., 1998). Below 2.5 mm, the RORSAT's droplets cannot be observed using the actual radar facilities.

Table 2

NUMBER OF RORSAT'S DROPLETS IN ORBIT: COMPARISON OF CODRM-99, MASTER-99 AND IDES-98 PREDICTIONS WITH DATA DERIVED FROM RADAR OBSERVATIONS

Particle Diameter ≥	CODRM-99 (01-01-1999)	MASTER-99 (01-08-1999)	IDES-98 (31-03-1998)	RADAR OBSERVATIONS
1 mm	2,765,569	286,550	148,428	-
2.5 mm	365,867	286,550	129,357	543,000
6.0 mm	49,969	42,899	78,428	43,000
1.0 cm	13,414	15,440	35,655	15,000
2.0 cm	2,061	2,017	2,413	2,000

Area-to-Mass Ratio

Sodium-potassium droplets aside, to relate the mass m (kg) and the cross-sectional area A (m^2) of space objects, the following relationship was adopted (Reynolds, 1990):

$$m = \begin{cases} 62.013A^{1.13} & A \geq 8.04 \cdot 10^{-5} \\ 2030.33A^{1.5} & A < 8.04 \cdot 10^{-5} \end{cases} \quad (6)$$

Object diameters were obtained assuming a spherical shape. For explosions and collisions, the mass of each fragment was used to compute a corresponding average cross-section by inverting Eq. (6); then, the actual area was randomly extracted from an appropriate log-normal distribution (Anselmo et al., 1996).

For the catalogued objects, when the mass was known with a reasonable level of confidence, the corresponding area was obtained using Eq. (6). On the other hand, if reasonable values for the mass were not available, the measured radar cross section was equated to the area and the corresponding mass was finally computed, again with Eq. (6).

Fragment Velocity Distribution

To find the orbits of the breakup fragments, a velocity distribution for the ejected material was needed. For explosions, the following relation was adopted (Reynolds, 1990):

$$\log(\overline{\Delta V}) = -0.0676(\log d)^2 - 0.804 \log d - 1.514 \tag{7}$$

where $\overline{\Delta V}$ is the average ejection velocity (km/s) and d is the fragment diameter (meters). To model the expulsion of the RORSAT's coolant droplets, the same formula was used, but the resulting velocity increment was reduced by an order of magnitude.

For collisional events, the following equation was instead adopted (Su, 1990):

$$\log\left(\frac{\overline{\Delta V}}{V_i}\right) = \begin{cases} A + B[\log(d/d_m)]^2 & d \geq d_m \equiv E^{1/3}/C \\ A & d < d_m \equiv E^{1/3}/C \end{cases} \tag{8}$$

where Vi is the relative impact velocity (km/s) and E is the impact kinetic energy (J). If the particle diameters are expressed in meters, the constants used assume the following numerical values:

$$A = -0.125$$
$$B = -0.0676$$
$$C = 8.01 \cdot 10^8$$

Known the average $\overline{\Delta V}$, the actual velocity increment of each fragment (ΔV) was obtained from the triangular distribution (Jehn, 1996):

$$\Delta V = \begin{cases} \overline{\Delta V}\left(0.1 + 0.6\sqrt{3y}\right) & 0.00 \leq y < 0.75 \\ \overline{\Delta V}\left(1.3 - 0.6\sqrt{1-y}\right) & 0.75 \leq y \leq 1.00 \end{cases} \tag{9}$$

where y is a random number between 0 and 1. Because all the breakup events were assumed isotropic, the velocity vector of each simulated fragment was obtained by adding to the velocity of the parent body a vector of magnitude ΔV and random direction. From the state

vector of the parent body at the breakup epoch, the computation of the orbit of each fragment produced was then easy.

DEBRIS PROPAGATION

The propagation to the environment reference epoch (January 1, 1999) of catalogued objects and debris clouds was performed using the FOP trajectory predictor (Pardini, 1993). The Fast Orbit Propagator (FOP) uses the variation of parameters theory and takes into account the main orbital perturbations, i.e. geo-potential harmonics up to the fifth order and degree, air drag (modified Jacchia-Roberts 1971 density model), moon and sun third body perturbations and solar radiation pressure with eclipses.

All the catalogued objects were individually propagated. On the other hand, the breakup fragments and the RORSAT's droplets were sampled according to their mass/diameter and only the sampled particles were actually propagated, with the implicit assumption that the orbital evolution of the debris represented by them would be the same.

For explosion and collision debris clouds, the following sampling factors were used, as a function of the debris mass m (kg):

- 1/1000 for $10^{-6} \leq m < 10^{-5}$
- 1/100 for $10^{-5} \leq m < 10^{-4}$
- 1/10 for $10^{-4} \leq m < 10^{-3}$
- 1/5 for $10^{-3} \leq m < 10^{-1}$
- 1/1 for $m \geq 0.1$

For the RORSAT's clouds of NaK droplets, the sampling factors used were, as a function of the particle diameter d (mm):

- 1/1000 for $1 \leq d < 2$
- 1/100 for $2 \leq d < 4$
- 1/10 for $4 \leq d < 6$
- 1/5 for $6 \leq d < 8$
- 1/1 for $d \geq 8$

In total, about 186,000 representative objects were propagated to the CODRM-99 reference epoch, for time intervals ranging from a few months to more than 37 years.

ORBITAL BREAKUPS

Following the first on-orbit fragmentation, the explosion of the *Transit 4A* rocket body on 29 June 1961, 154 breakups have been recorded until January 1, 1999 (reference epoch of the environment model). Generally, a fragmentation may result from either explosions or collisions, but explosions have been, so far, the primary contributors to the orbital debris environment. A variety of on-orbit explosive mechanisms is possible, including propulsion-related explosions, deliberate breakups, and catastrophic failure of internal components, such as batteries.

On the other hand, before January 1, 1999, only three collisional breakups have been reasonably confirmed:

- The American anti-satellite test in which a solar observation satellite, named *Solwind (P78-1)*, was destroyed by the impact with an air-launched miniature homing vehicle;
- The military satellite *USA 19*, which deliberately collided with its *Delta* upper stage during the *Delta 180* Strategic Defense Initiative orbital mission. But, probably, an explosive charge was detonated on-board one of the vehicles just before the collision occurred (Wilson, 1993);
- The first accidental hypervelocity collision between two catalogued objects, on July 24, 1996, when the stabilization boom of the French satellite *Cerise* was cut by a fragment produced in the breakup, on November 1986, of the *Ariane* third stage used to launch the *Spot 1* satellite. Despite this, the satellite recovered, the *Ariane* fragment seems intact, and only one new piece of debris was generated.

Breakup Classification

During the development of the ESA Meteoroid and Space Debris Terrestrial Environment Reference Model, an explosion intensity parameter B was introduced to fit the fragment mass distribution observed in ground tests and orbital breakups (Sdunnus, 1995). The parameter B has been estimated for most of the historical explosions considered in the present study (Sdunnus, 1996), so it was used to broadly classify the explosion intensity in three classes. For the events not included in the original MASTER list (Sdunnus, 1996), the intensity parameter was estimated by analogy with similar breakups. In other peculiar cases, the classification and the corresponding modeling of the events were based on additional information and analysis, taking into account radar observations (if available), orbital and size distribution of the resulting catalogued objects and possible breakup causes.

Low intensity explosions ($B < 1.3$) were simulated using the fragment mass distribution given in Eq. (1), high intensity explosions ($1.3 \leq B < 2.3$) with Eq. (3), and very high intensity explosions ($B \geq 2.3$) with Eq. (2). The *Solwind* breakup was the only one simulated using the collisional mass distribution given in Eq. (4); the *Delta 180* event was considered a low intensity explosion and, consequently, modeled using Eq. (1), while the collision involving *Cerise*, due to the nature of the event, did not need any modeling at all, having produced only one new detectable fragment. Table 3 summarizes the breakup classification and modeling.

Table 3

BREAKUP EVENTS CLASSIFICATION AND MODELING

EVENT CLASSIFICATION	NUMBER OF BREAKUPS
Low intensity explosions [Eq. (1)]	67
High intensity explosions [Eq. (3)]	66
Very high intensity explosions [Eq. (2)]	16
Collisions [Eq. (4)]	1
Collisions [no simulation]	1
Anomalous events [no simulation]	3
TOTAL	**154**

Fragmentation Events Included in the New Population

Table 4 shows the complete list of the breakup events simulated, together with the relevant parameters adopted. The following abbreviations apply:

- CATN: USSPACECOM Catalog Number;
- MASS: Breakup Mass [kg];
- CL: CNUCE Breakup Classification
  - **LI** = Low Intensity;
  - **HI-JP** = High Intensity;
  - **HI-E** = Very High Intensity;
  - **CO** = Collision;
  - **AE** = Anomalous Event (a debris loss was observed, but the parent objects seem still intact; on the basis of the information available, these events cannot be simulated as explosions or collisions);
- B_E : Breakup Epoch in yyddd.dddd;
- SMA: Parent object semimajor axis in km;
- ECC: Parent object eccentricity;
- INC: Parent object inclination in deg;
- RAN: Parent object right ascension of the ascending node in deg;
- AP: Parent object perigee argument in deg;
- MA: Parent object mean anomaly in deg.

Table 4

FRAGMENTATION EVENTS INCLUDED IN THE NEW DEBRIS POPULATION

SATELLITE NAME	CATN	MASS [kg]	CL	B_E yyddd.ddd	SMA [km]	ECC	INC [deg]	RAN [deg]	AP [deg]	MA [deg]
Transit 4A r/b [Ablestar Stage]	118	625	HI-E	61180.2555	7316.1	0.0070	66.88	96.15	296.38	206.16
Sputnik 29 r/b [Molnyia 8K78 3rd Stage]	443	1500	LI	62302.5000	6608.1	0.0055	65.09	320.83	89.97	157.59
Centaur AC-2 r/b [Centaur Stage]	694	4600	LI	63331.5000	7512.3	0.0873	30.40	163.86	106.25	150.12
Cosmos 50	919	4750	HI-JP	64310.5000	6589.2	0.0033	51.21	163.40	354.64	318.55
Cosmos 57	1093	5500	HI-JP	65053.4146	6672.1	0.0192	64.66	299.73	70.91	132.05
Cosmos 61-63 r/b [Kosmos 2nd Stage]	1270	1600	HI-JP	65074.7181	7420.6	0.1065	56.05	357.78	105.60	136.53
OV2-1-LCS 2 r/b [Titan Transtage]	1640	1500	HI-JP	65288.7639	7091.3	0.0071	32.20	84.67	194.12	115.81
Cosmos 95	1706	400	HI-JP	66015.5000	6743.2	0.0230	48.40	359.87	265.27	172.94
OPS 3031	2015	4	HI-E	66046.5000	6594.4	0.0117	96.59	147.42	127.02	68.79
Gemini 9 ATDA r/b [Saturn S-IVB Stage]	2188	3400	HI-JP	66166.5000	6641.6	0.0028	28.74	215.72	138.79	74.64
AS-203 r/b [Saturn S-IVB Stage]	2289	26000	LI	66186.8827	6581.6	0.0024	31.99	4.40	22.27	125.47
Cosmos U-1	2437	3000	HI-JP	66260.5000	6983.4	0.0638	49.59	342.60	78.99	326.43
Cosmos U-2	2536	3000	HI-JP	66306.5000	6893.8	0.0542	49.61	54.91	83.61	68.46
Cosmos 199	3099	5500	HI-JP	68024.5000	6658.0	0.0120	65.60	18.28	31.07	17.16
Apollo 6 r/b [Saturn S-IVB Stage]	3171	30000	LI	68104.4542	6663.8	0.0115	32.59	290.63	284.30	307.18
Cosmos 249	3504	1400	HI-JP	68294.6021	7703.4	0.1098	62.42	118.76	76.78	220.40
Cosmos 252	3530	1400	HI-JP	68306.1681	7715.1	0.1051	62.44	77.62	73.67	358.27
Cosmos 248	3503	1400	LI	68306.1750	6884.8	0.0042	62.35	77.29	305.17	165.99
Meteor 1-1 r/b [Vostok 8A92M Final Stage]	3836	1440	HI-JP	69087.7812	7031.9	0.0277	81.23	32.55	180.68	306.80
Intelsat 3 F-5 r/b [TE 364-4 Stage]	4052	1100	HI-JP	69207.1028	9231.8	0.2794	30.45	132.62	183.37	359.50
OPS 7613 r/b [Agena D Stage]	4159	600	HI-E	69277.6618	7380.6	0.0127	69.86	279.98	107.91	11.45
Nimbus 4 r/b [Agena D Stage]	4367	600	HI-E	70290.1368	7450.4	0.0013	99.83	204.07	180.33	127.93
Cosmos 374	4594	1400	HI-JP	70296.6340	7701.8	0.1040	62.94	129.10	60.50	285.58
Cosmos 375	4598	1400	HI-JP	70303.2500	7689.9	0.1031	62.92	104.70	56.03	8.06
Cosmos 397	4964	1400	HI-JP	71056.6049	7765.3	0.1055	65.75	355.11	50.94	9.70
Cosmos 462	5646	1400	HI-JP	71337.7021	7392.7	0.1072	65.64	297.12	54.13	4.84
Salyut 2 r/b [Proton 8K82K 3rd Stage]	6399	4000	LI	73093.9417	6597.9	0.0039	51.42	332.55	16.50	95.91
Cosmos 554	6432	6300	HI-JP	73126.3084	6634.6	0.0142	72.74	303.56	25.41	239.51
NOAA 3 r/b [Delta 100 2nd Stage]	6921	800*	HI-E	73362.3778	7881.9	0.0013	102.14	44.20	112.95	207.95
Landsat 1 r/b [Delta 100 2nd Stage]	6127	800*	HI-JP	75142.7688	7146.2	0.0200	98.30	196.22	40.09	287.14
Cosmos 699	7587	3000	HI-JP	75214.6826	6804.5	0.0012	64.90	273.26	308.47	232.89
NOAA 4 r/b [Delta 2914 2nd Stage]	7532	840*	HI-JP	75232.5465	7828.3	0.0018	101.55	277.87	69.15	165.80
Cosmos 758	8191	6200	HI-JP	75249.7959	6624.8	0.0124	67.12	188.66	69.01	326.55
Pageos	2253	55	HI-E	76020.9500	10555.6	0.1187	85.00	209.49	66.58	334.73
Cosmos 777	8416	3000	HI-JP	76025.5834	6812.6	0.0001	64.90	302.64	80.64	342.90
Landsat 2 r/b [Delta 2914 2nd Stage]	7616	840*	HI-JP	76170.2909	7202.1	0.0121	97.76	95.58	142.68	353.54
Cosmos 844	9046	6700	HI-JP	76207.7209	6638.6	0.0146	67.21	151.39	71.68	52.34

Cosmos 886	9634	1400	HI-JP	76362.7778	7823.0	0.1084	65.72	336.91	198.79	113.30
Cosmos 884	9614	6300	HI-JP	76364.5000	6608.0	0.0106	65.00	228.85	117.59	11.87
Cosmos 862	9495	1250	LI	77074.5389	26586.8	0.7305	63.28	97.29	318.67	13.00
Cosmos 838	8932	3000	HI-JP	77137.4292	6805.6	0.0012	65.17	129.36	299.44	250.85
Himawari 1 r/b [Delta 2914 2nd Stage]	10144	840*	HI-JP	77195.6749	7663.3	0.0977	28.90	270.58	52.56	86.84
Cosmos 839	9011	650	HI-JP	77272.3035	7917.0	0.0705	66.01	82.06	351.04	231.73
Cosmos 931	10150	1250	LI	77297.5000	26537.4	0.7330	62.74	304.27	318.79	7.34
Cosmos 970	10531	1400	HI-JP	77355.7153	7419.3	0.0138	65.69	281.68	114.60	203.92
NOAA 5 r/b [Delta 2914 2nd Stage]	9063	840*	HI-JP	77358.4812	7889.1	0.0016	102.12	42.09	54.32	263.71
Cosmos 903	9911	1250	LI	78159.5000	26556.8	0.7103	63.32	114.88	319.86	107.57
Ekran 2	10365	1750	LI	78174.5000	42183.7	0.0001	8.93	315.03	34.69	211.58
Cosmos 1030	11015	1250	LI	78283.5000	26590.9	0.7338	62.78	335.62	318.39	226.22
Cosmos 880	9601	650	HI-JP	78331.7104	6962.6	0.0042	65.88	10.38	311.18	314.26
Cosmos 917	10059	1250	LI	79089.6563	26596.0	0.6973	63.04	155.63	322.53	352.18
Cosmos 1124	11509	1250	LI	79252.1042	26565.5	0.7375	62.78	287.48	318.37	16.50
Cosmos 1094	11333	3000	LI	79260.4437	6769.8	0.0009	64.88	271.12	327.85	275.28
Cosmos 1109	11417	1250	LI	80046.5000	26569.5	0.7230	63.51	104.38	318.53	172.91
CAT r/b [Ariane 1 3rd Stage]	11659	1400	LI	80106.5000	22990.5	0.7151	18.07	93.17	279.47	155.02
Cosmos 1174	11765	1400	HI-JP	80109.3097	7395.7	0.0858	65.96	251.07	248.42	160.94
Landsat 3 r/b [Delta 2914 2nd Stage]	10704	840*	HI-JP	81027.1889	7282.6	0.0009	99.01	68.58	127.76	145.76
Cosmos 1261	12376	1250	LI	81121.5000	26571.3	0.7360	62.87	278.51	316.59	117.43
Cosmos 1191	11871	1250	LI	81134.5000	26562.9	0.7170	62.63	197.92	319.70	314.13
Cosmos 1167	11729	3000	LI	81196.3896	6779.8	0.0059	65.02	173.78	245.21	126.18
Cosmos 1275	12504	800	HI-E	81205.9938	7362.5	0.0044	83.11	118.98	127.62	302.30
Cosmos 1305 r/b [Molniya 8K78M 3rd Stage]	12827	1100	LI	81254.5000	13577.7	0.4852	62.97	70.77	286.57	286.53
Cosmos 1247	12303	1250	LI	81293.5000	26559.1	0.7230	62.95	213.69	318.47	241.71
Cosmos 1285	12627	1250	LI	81325.5000	26787.2	0.7350	63.03	248.93	317.15	238.55
Nimbus 7 r/b [Delta 2914 2nd Stage]	11081	840*	LI	81360.5000	7320.3	0.0020	99.13	277.15	68.70	16.04
Cosmos 1220	12054	3000	HI-JP	82171.7625	7103.7	0.0219	64.92	329.94	0.18	190.31
Cosmos 1306	12828	3000	LI	82193.9757	6769.4	0.0011	65.06	40.96	302.47	333.35
Cosmos 1260	12364	3000	HI-JP	82222.9826	6976.4	0.0211	65.15	45.11	296.08	184.34
Cosmos 1286	12631	3000	LI	82272.2223	6689.7	0.0007	65.14	132.47	263.77	155.20
Cosmos 1423 r/b [Molniya 8K78M 3rd Stage]	13696	1100	HI-JP	82342.6167	6707.6	0.0152	62.82	315.84	58.28	220.38
Cosmos 1217	12032	1250	LI	83043.5000	26558.1	0.7022	65.20	257.98	274.70	165.47
Cosmos 1481	14182	1250	LI	83190.5000	26301.5	0.7340	62.93	165.82	318.12	109.51
Cosmos 1355	13150	3000	HI-JP	83220.9799	6754.8	0.0015	64.87	276.37	307.11	17.07
Cosmos 1456	14034	1250	LI	83225.0000	26518.7	0.7315	63.44	79.51	319.95	3.75
Cosmos 1405	13508	3000	HI-JP	83354.5104	6701.4	0.0016	65.16	124.63	346.08	223.42
Cosmos 1317	12933	1250	LI	84028.5000	26563.3	0.7099	62.61	218.66	324.38	37.79
Westar 6 r/b [PAM-D Upper Stage]	14694	30**	LI	84034.9063	6689.5	0.0004	28.54	156.37	5.23	354.11
Palapa B2 r/b [PAM-D Upper Stage]	14693	30**	LI	84037.6666	6663.6	0.0002	28.59	135.79	323.34	39.95
Astron Ullage Motor [Proton SOZ]	13902	55	LI	84247.8493	7102.6	0.0702	51.72	90.54	248.48	312.01
Cosmos 1461	14064	3000	HI-JP	85133.0646	7104.9	0.0215	65.00	331.39	232.32	137.76
Cosmos 1654	15734	6700	LI	85172.4493	6617.5	0.0094	64.86	359.26	51.70	317.38
P-78/Solwind	11278	850	CO	85256.8632	6906.0	0.0033	97.63	182.21	96.14	300.96
Cosmos 1375	13259	650	HI-JP	85294.1618	7372.4	0.0013	65.80	349.15	67.51	21.41
Cosmos 1691	16139	220	HI-JP	85326.3611	7790.0	0.0007	82.56	341.08	95.56	52.42
Cosmos 1714 r/b [Zenit 2nd Stage]	16439	9000	LI	85362.5000	6877.1	0.0484	71.00	282.00	0.00	178.00
NOAA 8	13923	1000	LI	85364.4201	7192.3	0.0010	98.70	32.30	190.24	57.79
Cosmos 1588	15167	3000	HI-JP	86054.7847	6799.6	0.0013	64.83	246.84	296.20	95.89
USA 19	16937	930	LI	86248.7445	6872.3	0.0407	39.16	39.27	12.59	8.39
USA 19 r/b	16938	1455	LI	86248.7445	6798.6	0.0291	22.82	19.47	39.05	359.77
Spot 1 r/b	16615	1400	HI-JP	86317.8194	7193.3	0.0027	98.76	30.15	43.64	325.69

[Ariane 1 3rd Stage]										
Cosmos 1278	12547	1250	LI	86335.5000	26553.7	0.6599	66.94	287.49	291.95	214.72
Cosmos 1682	16054	3000	LI	86352.8451	6807.2	0.0075	64.93	333.86	49.98	285.79
Cosmos 1813	17297	6300	HI-JP	87029.2465	6762.2	0.0044	72.62	255.47	167.44	281.38
Cosmos 1866	18184	6700	LI	87207.6521	6580.8	0.0083	67.36	98.11	65.26	230.50
Aussat K3/ECS 4 r/b [Ariane 3 3rd Stage]	18352	1200	LI	87262.5000	24767.9	0.7333	6.95	175.44	181.96	222.02
Cosmos 1769	16895	3000	LI	87264.5035	6755.0	0.0090	65.19	119.66	290.19	325.56
Cosmos 1646	15653	3000	LI	87324.0632	6775.7	0.0009	64.83	285.30	237.68	215.82
Cosmos 1823	17535	1500	HI-JP	87351.7354	7878.6	0.0025	73.59	183.86	194.54	2.19
Cosmos 1656 Ullage Motor [SOZ]	15773	55	HI-JP	88005.0743	7211.5	0.0025	66.50	198.74	264.79	183.53
Cosmos 1906	18713	6300	HI-JP	88031.4646	6629.3	0.0023	82.38	253.48	125.54	63.89
Cosmos 1916	18823	6700	LI	88058.1972	6565.3	0.0067	64.62	263.87	57.14	18.24
Cosmos 1045 r/b [Tsyklon 3rd Stage]	11087	1360	HI-JP	88130.5125	8069.5	0.0020	82.55	353.47	74.28	134.16
Cosmos 2030	20124	6700	LI	89209.1771	6556.3	0.0055	67.37	88.57	63.45	354.07
Cosmos 2031	20136	6500	LI	89243.7854	6683.2	0.0101	50.35	242.21	58.58	61.14
Fengyun 1-2 r/b [CZ-4A Final Stage]	20791	1000	HI-JP	90277.8430	7265.0	0.0013	98.76	288.90	131.78	137.17
Cosmos 2101	20828	6500	LI	90334.7222	6614.9	0.0070	64.70	346.52	147.19	331.10
USA 68 r/b [TE-M-364-15 Upper Stage]	20978	855	HI-JP	90335.6736	7167.4	0.0081	98.87	3.43	6.38	165.74
Cosmos 1519-21 Ullage Motor [SOZ]	14608	55	HI-JP	91035.1333	15952.4	0.5781	52.14	131.15	316.97	201.01
Cosmos 2125-32 r/b [Kosmos 2nd Stage]	21108	1435	HI-JP	91064.5729	7970.6	0.0159	74.10	163.40	241.50	72.96
Nimbus 6 r/b [Delta 2914 2nd Stage]	7946	840*	HI-JP	91121.3722	7473.4	0.0015	99.46	336.90	103.67	326.65
Cosmos 2163	21741	6500	LI	91340.8480	6597.9	0.0060	64.91	36.10	138.81	337.06
Cosmos 1710-12 Ullage Motor [SOZ]	16446	55	LI	91363.3771	16143.4	0.5650	65.43	37.16	243.88	337.53
OV2-5 r/b [Titan Transtage]	3432	1500	HI-JP	92052.3965	41835.7	0.0085	11.99	22.27	75.71	246.64
Cosmos 2054 Ullage Motor [SOZ]	20399	55	LI	92183.5000	20353.4	0.6704	46.95	305.19	319.33	9.57
Cosmos 1603 Ullage Motor [SOZ]	15338	55	HI-JP	92249.6188	7217.3	0.0011	66.54	352.31	50.64	181.42
Gorizont 17 Ullage Motor [SOZ]	19771	55	LI	92353.5000	15253.0	0.5693	46.48	264.90	354.82	10.57
Cosmos 2227 r/b [Zenit 2nd Stage]	22285	9000	HI-JP	92361.3181	7226.7	0.0015	70.85	226.79	83.72	347.99
Gorizont 18 Ullage Motor [SOZ]	20116	55	LI	93012.5000	21874.5	0.6976	46.56	212.03	47.85	309.00
Cosmos 2225	22280	6500	LI	93049.7889	6610.9	0.0043	65.09	91.81	107.46	7.08
Cosmos 2237 r/b [Zenit 2nd Stage]	22566	9000	LI	93087.3028	7223.1	0.0003	70.76	260.31	75.22	8.15
Telecom 2B/Inmarsat 2 r/b [Ariane 4 3rd Stage]	21941	1800	LI	93111.5000	24318.4	0.7245	3.44	223.61	111.79	169.56
Cosmos 2243	22641	6700	HI-JP	93117.4473	6606.9	0.0055	70.55	56.77	82.07	349.81
Cosmos 2259	22716	6700	HI-JP	93206.5000	6626.3	0.0114	67.13	134.47	68.98	113.68
Cosmos 1484	14207	30***	HI-JP	93291.5027	6947.4	0.0027	97.35	317.36	328.95	22.85
Cosmos 2262	22789	6500	LI	93352.2993	6602.2	0.0075	64.75	208.49	69.53	21.43
Clementine r/b [Titan II G]	22974	2860	HI-JP	94038.7215	6610.4	0.0033	67.18	45.80	135.08	113.33
OPS 9331-34 r/b [Titan Transtage]	2868	1500	HI-JP	94039.5000	39840.6	0.0053	11.7	307.63	129.58	109.93
Astra 1B/MOP 2 r/b [Ariane 4 3rd Stage]	21141	1760	LI	94117.6377	20927.7	0.6824	6.74	139.15	177.67	0.50
Cosmos 2133 Ullage Motor [SOZ]	21114	55	LI	94127.3958	17394.5	0.6204	46.83	109.38	161.43	211.96
Cosmos 2204-06 Ullage Motor [SOZ]	22067	55	HI-JP	94312.5000	16135.6	0.5749	64.85	65.20	316.80	217.05
RS-15 r/b	23440	1000	HI-JP	94360.2688	8418.2	0.0190	64.80	83.74	283.80	273.88

[Briz]										
ETS-VI r/b [H-II 2nd Stage]	23231	3000	LI	95090.9300	18543.1	0.6490	28.50	7.08	16.22	0.00
Elektro Ullage Motor [SOZ]	23338	55	HI-E	95131.5000	24188.1	0.7299	46.71	200.00	300.00	200.00
Cosmos 2282 Ullage Motor [SOZ]	23174	55	HI-E	95294.5000	23990.2	0.7222	46.97	157.14	127.94	322.60
Gorizont 22 Ullage Motor [SOZ]	20957	55	HI-E	95348.5000	12911.7	0.4944	46.50	140.58	117.08	93.62
Raduga 33 r/b [Proton Block DM]	23797	3400	LI	96050.6243	24798.6	0.7321	48.58	282.00	0.00	178.00
Eutelsat-II-F2 r/b [Ariane 4 3rd Stage]	21057	1760	LI	96122.5000	21974.2	0.6990	6.64	96.14	149.23	37.77
STEP M2 r/b [Pegasus HAPS]	23106	97	HI-E	96155.6375	7081.8	0.0153	81.97	342.00	210.00	35.00
Cerise	23606	50	CO	96205.4083	7049.1	0.0017	98.01	141.79	48.51	271.19
Cosmos 1883-85 Ullage Motor [SOZ]	18374	55	HI-E	96335.5000	16121.4	0.5839	64.90	299.57	180.62	312.06
Ekran 7 Ullage Motor [SOZ]	18719	55	HI-E	97142.5000	17985.5	0.6285	46.63	253.04	349.71	162.72
Cosmos 2313	23596	3000	AE	97177.1229	6644.0	0.0077	65.02	342.08	234.68	175.35
Cosmos 2343	24805	6500	LI	97259.9200	6633.0	0.0045	64.85	1.15	113.60	316.27
Cosmos 1869	18214	1900	AE	97331.0160	6997.0	0.0021	82.51	97.79	115.24	111.78
Cosmos 1172	11758	1250	LI	97357.5000	9515.1	0.3214	61.81	113.36	248.22	145.54
Asiasat 3 r/b [Proton Block DM3]	25129	3400	LI	97359.2431	24510.5	0.7288	51.45	92.06	1.02	358.60
Molniya 3-16	12512	1600	LI	97036.5000	10256.9	0.3698	62.10	87.06	273.44	149.54
Electron 1 r/b [Vostok 8A92 2nd Stage]	751	1440	LI	97042.5000	7019.2	0.0811	56.23	135.26	67.55	2.05
Meteor 2-16 r/b [Tsyklon 3rd Stage]	18313	1360	HI-JP	98046.9333	7328.5	0.0010	82.55	230.97	335.00	94.03
Astra 1A r/b [Ariane 4 3rd Stage]	19689	1760	LI	98048.5243	24724.5	0.7254	7.34	23.80	248.17	181.98
COMETS r/b [H-2 2nd Stage]	25176	3000	AE	98052.5000	7443.2	0.1098	30.05	294.30	194.57	118.74
Cosmos 2109-2111 Ullage Motor [SOZ]	21013	55	HI-E	98073.5000	16135.5	0.5725	65.08	306.45	216.72	150.68
Cosmos 1987-1989 Ullage Motor [SOZ]	19755	55	HI-E	98215.5000	16075.5	0.5821	64.92	16.77	182.60	12.04
Cosmos 1650-1652 Ullage Motor [SOZ]	15714	55	HI-E	98333.5000	15852.0	0.5769	52.04	344.46	209.69	94.77

The masses used are those adopted at the 14th IADC meeting (Johnson, 1997), unless otherwise specified. For later fragmentation events, the values indicated in the NASA's History of On-Orbit Satellite Fragmentations were used (Johnson et al., 1998). Different information sources were utilized in the cases described below.

* Delta 100 and Delta 2000 2nd stage: the masses recommended by P. Anz-Meador (personal communication, 1999) have been used.

** The satellites Palapa B2 and Westar 6 were deployed from the Space Shuttle STS-41B in February 1984, but both were stranded in a low orbit by the failure of their PAM-D GTO insertion stage. Both satellites were retrieved and returned to earth for renovation on the STS-51A mission. If the PAM-D upper stages had been totally disrupted during the firing, the recovered satellites should have been damaged, but this was not the case. Both PAM-D stages that are still observed by the US Space Command as intact objects suffered probably only the loss of nozzle pieces. Anyway,

although some debris was originated by the stage fragmentation, perhaps only a very small fraction of the body suffered a breakup. For this reason, it was supposed that a small mass, equal approximately to 30 kg, exploded.

*** The breakup of the satellite Cosmos 1484 was discussed by McKnight (1994). The reference quotes: "Adding some mystery to the breakup are the results of an attempt to image the primary remnant of Kosmos 1484 by the German FGAN radar on 1 December [1993]. Data from a long slant range, low elevation pass indicates that the spacecraft remains virtually intact with no apparent rupture of the main body or solar panels". Taking into account this information, only a small fraction of the satellite mass suffered a breakup. This mass was extrapolated from the Cosmos 1484 "Family" Size Distribution observed by the Haystack radar (Stansbery et al., 1996, p. 77). The extrapolation consisted in roughly reproducing the Haystack distribution through the simulation of the explosion of a mass to be determined. The results gave a mass equal to about 30 kg.

CATALOGUED OBJECTS

The catalogued objects were provided by ESA/ESOC. The file contained 8508 objects in orbit around the earth, identified by the following parameters:

1. Semimajor axis;
2. Eccentricity;
3. Inclination;
4. Radar cross-section;
5. Mass;
6. Diameter.

Mass and diameter were available only for a small subset of the objects.

The spatial density of the catalogued objects is shown in Figures 1 and 2, as a function of their altitude.

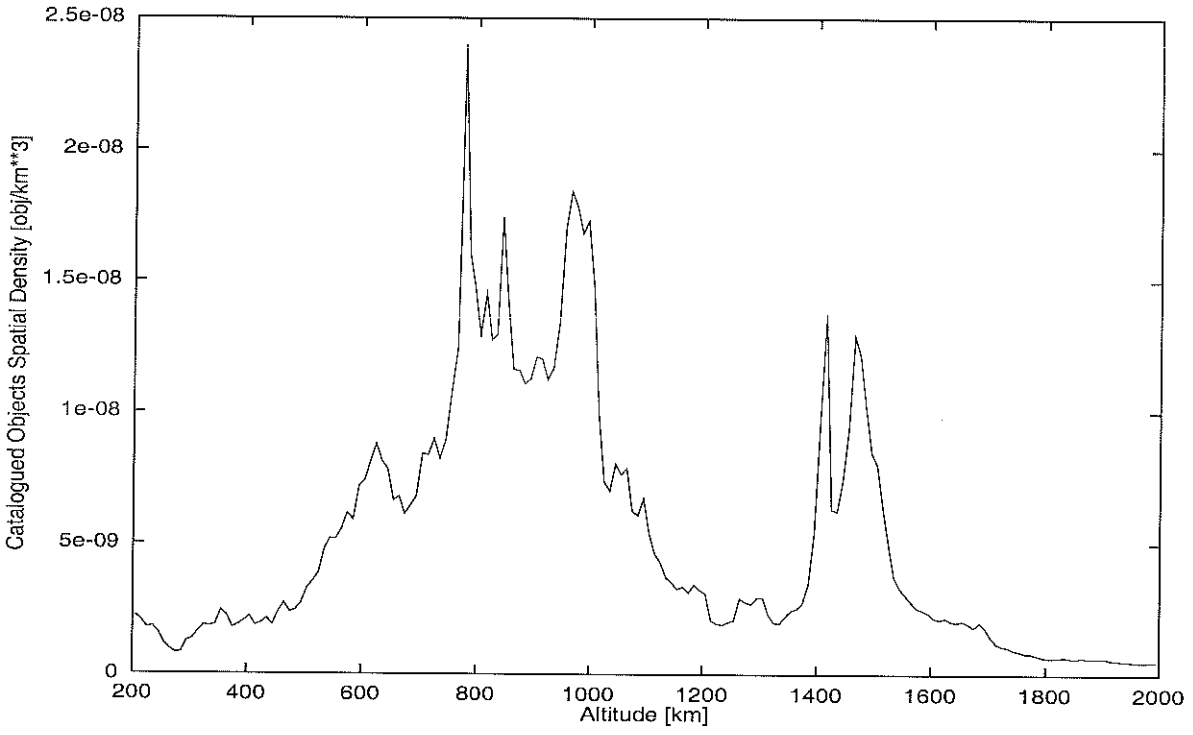

Figure 1. Catalogued Objects Spatial Density Below 2000 km

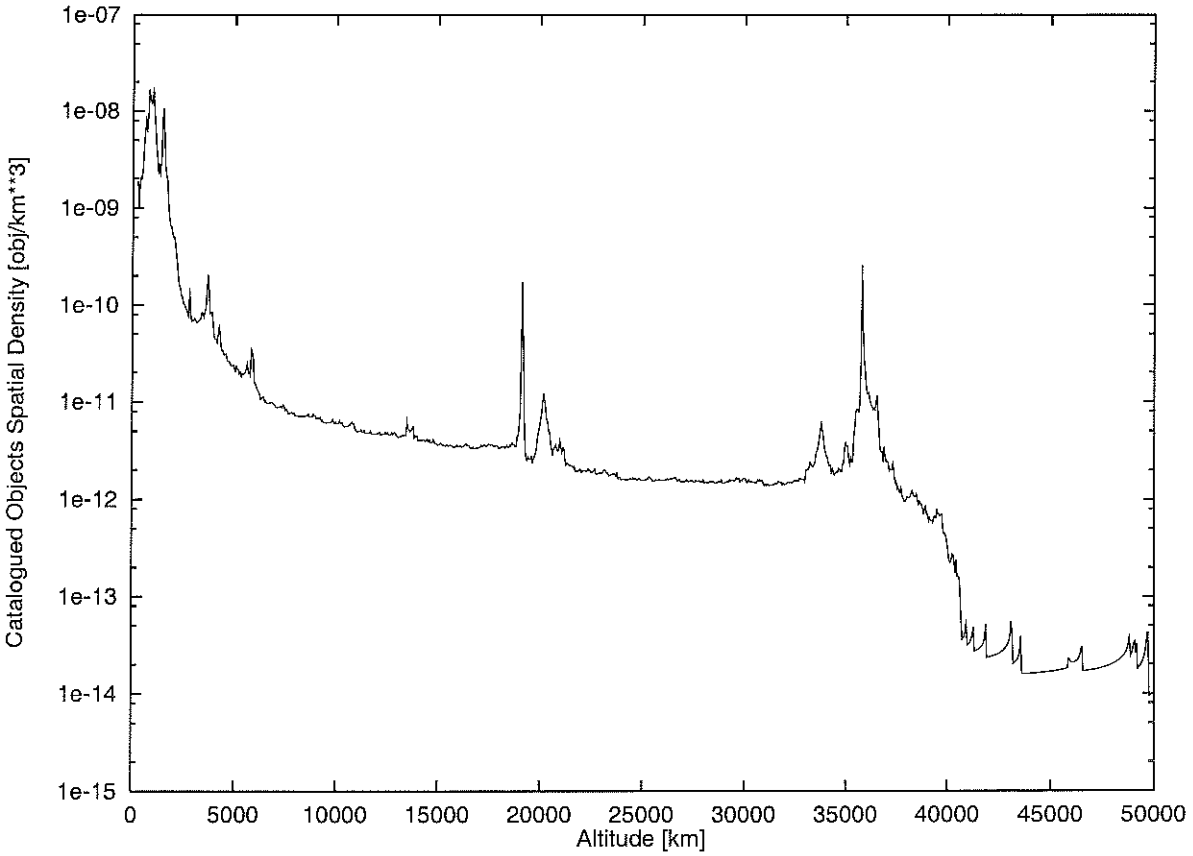

Figure 2. Catalogued Objects Spatial Density Below 50000 km

THE NEW ORBITAL DEBRIS POPULATION

The simulated debris clouds, produced by 150 fragmentation (of the 154 breakup events listed in Table 4, four events were not simulated: the Cerise collision, producing only a catalogued fragment, and the three breakups classified as anomalous events) and 16 RORSAT leakage events considered in the present modeling effort, were propagated to the chosen reference epoch, including all the particles larger than 1 mm. All these objects were retained up to the size of 15 cm. Above this threshold, an appropriate number of simulated debris was randomly sorted out to compensate the incompleteness of the catalog. In between 15 and 20 cm, one out of five objects was retained, while above 20 cm the additional particles selected were one out of fifteen. This choice was consistent with a catalog incompleteness close to 90% in between 10 and 15 cm, 50% in between 15 and 20 cm, 10% in between 20 and 50 cm.

The new debris population was obtained by merging the artificial debris environment so computed with the catalogued population provided by ESA/ESOC. The lower size limit is 1 mm, and the maximum altitude considered is 100,000 km. The cumulative number of objects as a function of the diameter is given in Table 5 (full population) and in Table 6 (below 2000 km).

The spatial density distribution as a function of the altitude is shown in Figures 3 and 4, for artificial debris larger than 1 mm, 1 cm, and 10 cm.

Table 5

CUMULATIVE NUMBER OF OBJECTS LARGER THAN A GIVEN DIAMETER

Diameter [≥]	Cumulative Number of Objects
1 mm	21 782 098
5 mm	405 678
7 mm	213 163
1 cm	117 303
2 cm	52 179
5 cm	26 226
10 cm	15 667
20 cm	7 473

Table 6

CUMULATIVE NUMBER OF OBJECTS LARGER THAN A GIVEN DIAMETER BELOW THE ALTITUDE OF 2000 km

Diameter [≥]	Average Number of Particles	Number of Crossing Particles
1 mm	7 135 847	19 700 225
5 mm	242 188	365 815
7 mm	133 955	190 050
1 cm	75 032	102 375
2 cm	30 939	42 882
10 cm	9 553	12 844
20 cm	5 296	6 246

Population Files Structure

In order to be used as initial conditions for the SDM software, two debris population files have been generated. The first includes catalogued objects and fragmentation debris, the second RORSAT's sodium-potassium droplets. Both the files have the same column structure:

1. Object index;
2. Sampling factor;
3. Mass [kg];
4. Cross-section [m^2];
5. Diameter [m];
6. Semimajor axis [km];
7. Eccentricity;
8. Inclination [deg].

The object indices used, according to the overall SDM upgrade plan, were the following:

- Catalogued objects: 150,000
- RORSAT's droplets: 120,000
- Collision fragment: 110,000
- Generic fragment: 140,000

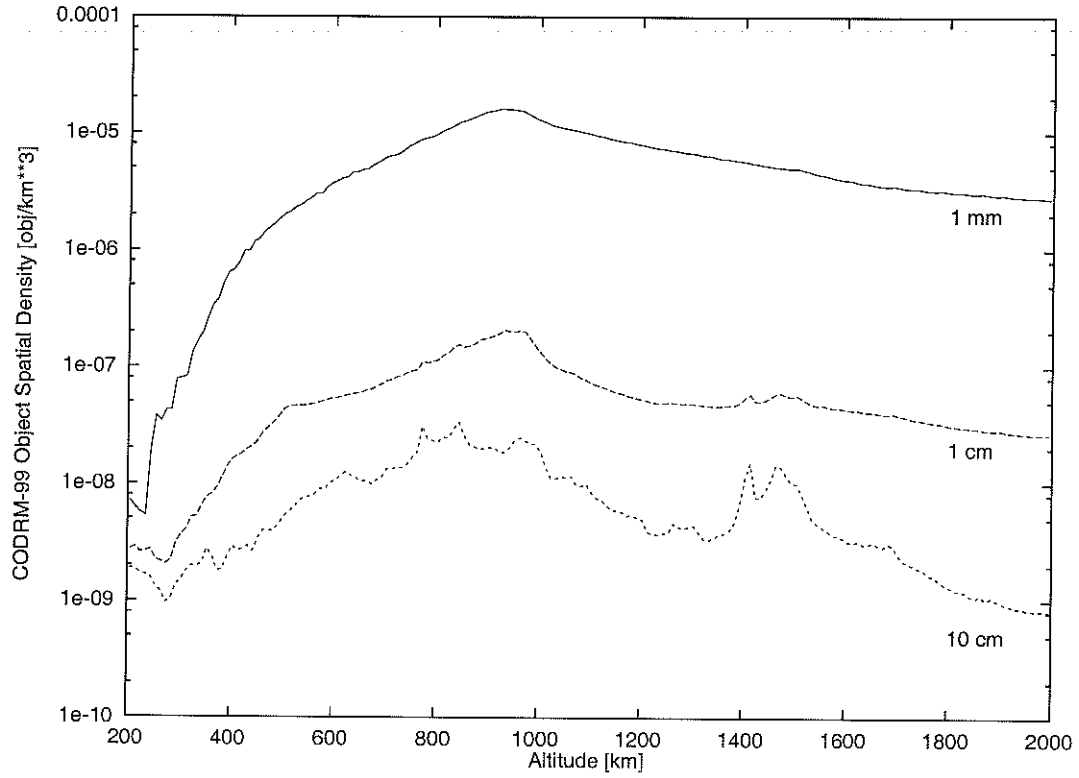

Figure 3. Spatial Density Below 2000 km for Objects with Diameters ≥ 1 mm, 1 cm, 10 cm

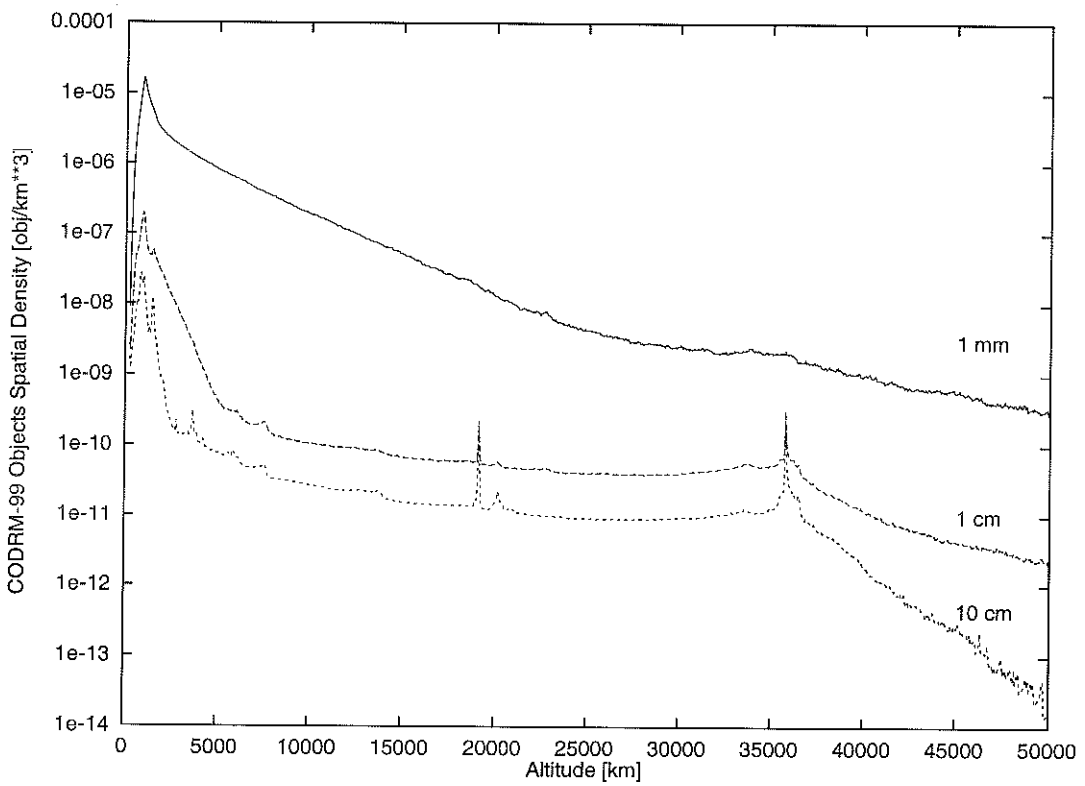

Figure 4. Spatial Density Below 50000 km for Objects with Diameters ≥ 1 mm, 1 cm, 10 cm

Comparison with Other Models

To assess the validity of the new CNUCE Orbital Debris Reference Model results, the spatial density of the CODRM-99 particles (larger than 1 mm, 1 cm and 10 cm) below 2000 km was compared with that computed by the MASTER-99, IDES-98 and ORDEM96 models. The files including the objects spatial density - as a function of altitude - at the reference epoch of the MASTER-99 (August 1, 1999) and IDES-98 (March 31, 1998) models were provided by Ruediger Jehn (ESA/ESOC). ORDEM96 does not provide the objects spatial density, but an estimation of the total cross sectional area flux as a function of altitude, inclination and solar flux at 10.7 cm. So, the flux was computed for the year 1999, by selecting an average orbital inclination of 50 degrees and a solar flux of $130 \cdot 10^{-22}$ Wm^{-2} Hz^{-1}. The spatial density was then derived from the flux, by assuming an average debris relative velocity of 10 km/sec.

Figures 5, 6, and 7 show the spatial density versus altitude of the objects larger than 1 mm, 1 cm and 10 cm, respectively, as derived by the considered models. Unlike the CODRM-99 and IDES-98 models, MASTER-99 also includes the slag particles generated by the solid rocket motors. For this reason, a distinction was introduced in the figures to distinguish between the complete model (MASTER-99) and the model without slag particles (MASTER-99_no_srm).

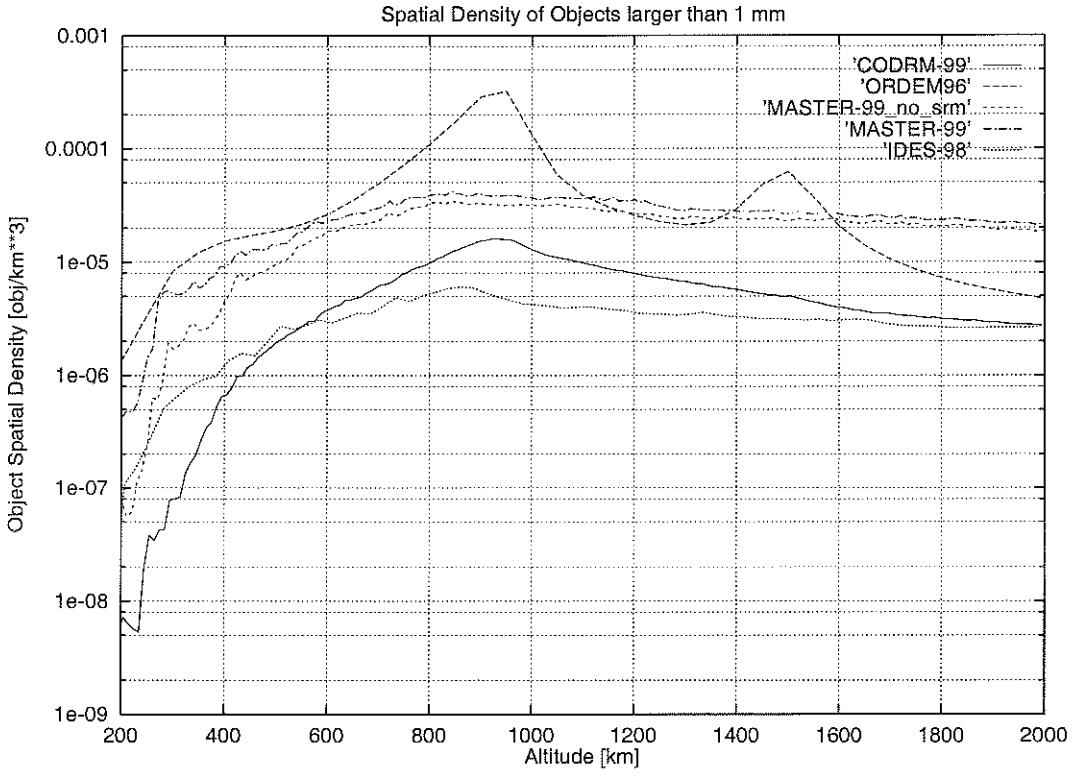

Figure 5. Comparison of Spatial Density Below 2000 km for Objects with Diameters ≥ 1 mm

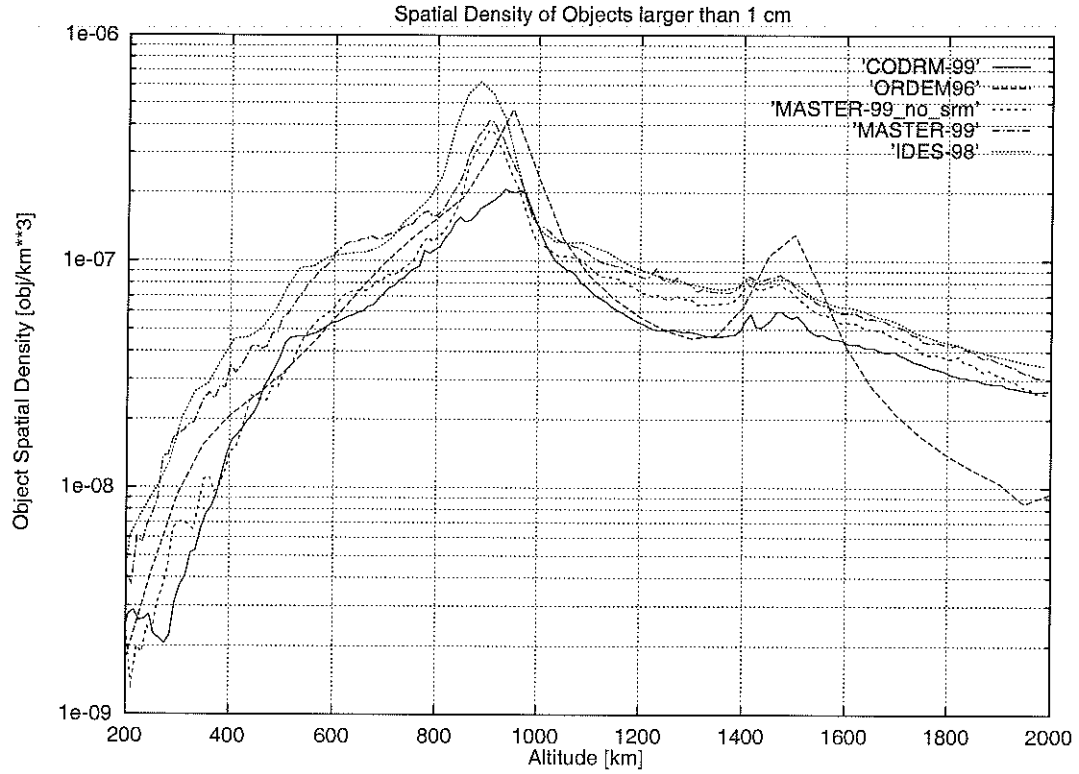

Figure 6. Comparison of Spatial Density Below 2000 km for Objects with Diameters ≥ 1 cm

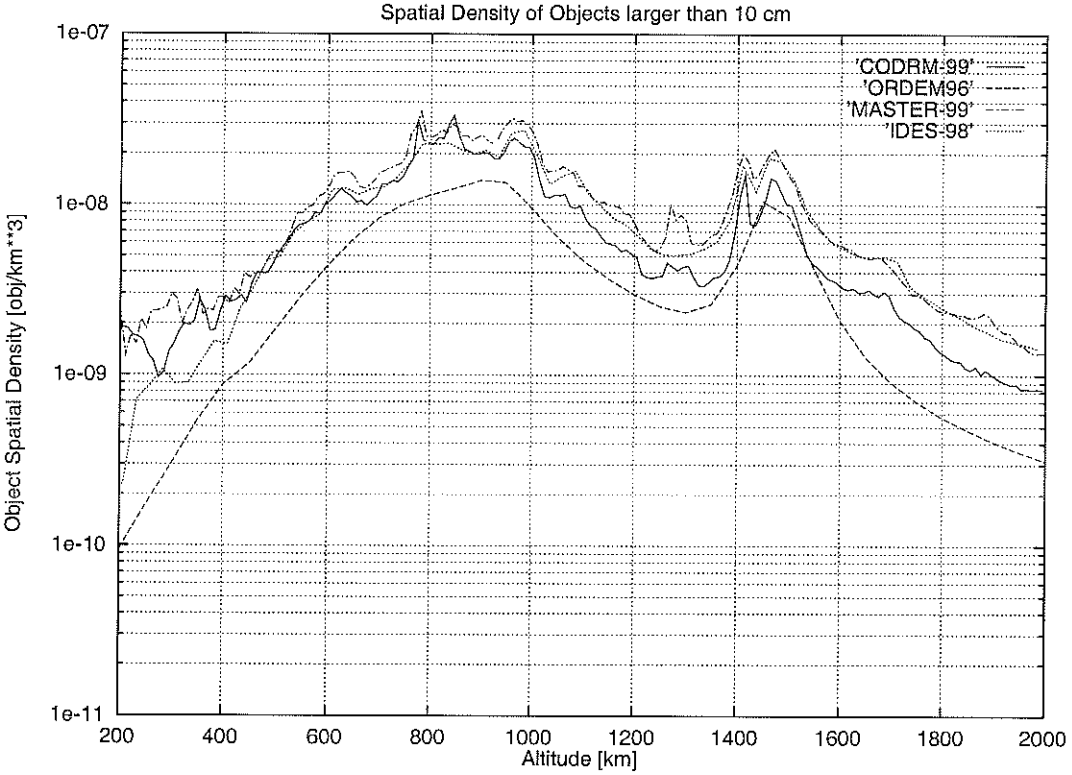

Figure 7. Comparison of Spatial Density Below 2000 km for Objects with Diameters ≥ 10 cm

REFERENCES

1. Anselmo, L., A. Cordelli, P. Farinella, C. Pardini and A. Rossi, Final Report, *Study on Long Term Evolution of Earth Orbiting Debris, ESA/ESOC Contract No. 10034/92/D/IM(SC)*, Consorzio Pisa Ricerche, Pisa, Italy, April 1996.
2. Goldstein, R.M., S.J. Goldstein, and D.J. Kessler, Radar Observation of Space Debris, *Planetary and Space Sciences*, **46**, 1998, pp. 1007-1013.
3. Jehn, R., Modelling Debris Clouds, Shaker Verlag, Aachen, Germany, 1996.
4. Johnson, N.L., Known Earth Satellite Breakups, *Proceedings of the 14th Inter-Agency Space Debris Coordination Meeting*, Annex WG4-A3, ESA/ESOC, Darmstadt, Germany, March 20-21, 1997.
5. Johnson, N.L., A. Bade, P. Eichler, E. Cizek, S. Robertson and T. Settecerri, History of On-Orbit Satellite Fragmentations, Eleventh Edition, *JSC-28383*, Johnson Space Center, NASA, Houston, USA, July 31, 1998.
6. Kessler, D.J., J. Zhang, M.J. Matney, P. Eichler, R.C. Reynolds, P.D. Anz-Meador and E.G. Stansbery, A Computer-Based Orbital Debris Environment Model for Spacecraft Design and Observations in Low-Earth Orbit, *NASA TM-104825*, November 1996.
7. Klinkrad, H., J. Bendisch, H. Sdunnus, P. Wegener and R. Westerkamp, An Introduction to the 1997 ESA MASTER Model, *Proceedings of the Second European Conference on Space Debris*, ESA SP-393, 1997, pp. 217-224.
8. McKnight, D.S., Breakup in Review: Kosmos 1484 (1983-75A), *Orbital Debris Monitor*, **7**, No. 1, 1994, p. 18.
9. Pardini, C., Development of a Fast Orbit Propagator, *Study Note of Work Package 3100, Study on Long Term Evolution of Earth Orbiting Debris, ESA/ESOC Contract No. 10034/92/D/IM(SC)*, Consorzio Pisa Ricerche, Pisa, Italy, September 1993.
10. Pardini, C., Development of a Single Fragmentation Event Simulator (CLDSIM), *Study Note of Work Package 3600, Study on Long Term Evolution of Earth Orbiting Debris, ESA/ESOC Contract No. 10034/92/D/IM(SC)*, Consorzio Pisa Ricerche, Pisa, Italy, September 1995.
11. Pardini, C., The Past On-Orbit Satellites and Rocket Bodies Fragmentations, *CNUCE/CNR Technical Report C97-020*, Pisa, Italy, December 1, 1997.
12. Pardini, C., A. Cordelli, A. Rossi, L. Anselmo and P. Farinella, The Contribution of Past Fragmentation Events to the Uncatalogued Orbital Debris Population, in *Astrodynamics 1995, Advances in the Astronautical Sciences*, **90**, Univelt Inc., San Diego, California, USA, 1995, pp. 809-828.
13. Pardini C., L. Anselmo, A. Rossi, A. Cordelli, P. Farinella, The 1997.0 CNUCE Orbital Debris Reference Model, in *Spaceflight Mechanics 1998, Advances in the Astronautical Sciences*, **99**, Univelt Inc., San Diego, California, USA, 1998, pp. 1041-1058.

14. Reynolds, R.C., Review of Current Activities to Model and Measure the Orbital Debris Environment in Low-Earth-Orbit, *Advances in Space Research*, **10**, 1990, pp. 359-372.
15. Reynolds, R.C., Documentation of Program EVOLVE: A Numerical Model to Compute Projections of the Man-made Orbital Debris Environment, *SPC Report No. OD91-002-U-CSP*, System Planning Corp., February 15, 1991.
16. Sdunnus, H., Final Report, *Meteoroid and Space Debris Terrestrial Environment Reference Model, ESA/ESOC Contract No. 10453/93/D/CS*, July 1995.
17. Sdunnus, H., MASTER Log of On-Orbit Fragmentation Events, *MAS Working Paper No. 382*, ESA/ESOC, Darmstadt, Germany, April 1996.
18. Stansbery, E. and T.J. Settecerri, A Comparison of Haystack and HAX Measurements of the Orbital Debris Environment, *Proceedings of the Second European Conference on Space Debris,* ESOC, Darmstadt, Germany, 17-19 March, 1997, ESA SP-393, May 1997, pp. 59-63.
19. Stansbery, E.G., T.J. Settecerri, M.J. Matney, J. Zhang and R. Reynolds, Haystack Radar Measurements of the Orbital Debris Environment: 1990-1994, *JSC-27436*, Johnson Space Center, NASA, Houston, April 20, 1996.
20. Su, S.Y., The Velocity Distribution of the Collisional Fragments and Its Effect on the Future Space Debris Environment, *Advances in Space Research*, **10**, 1990, pp. 389-392.
21. Su, S.Y., and D.J. Kessler, Contribution of Explosion and Future Collision Fragments to the Orbital Debris Environment, *Advances in Space Research*, **5**, 1985, pp. 25-34.
22. Walker, R., S. Hauptmann, R. Crowther, H. Stokes and A. Cant, Introducing IDES: Characterising the Orbital Debris Environment in the Past, Present and Future, in *Spaceflight Mechanics 1996*, Advances in the Astronautical Sciences Series, Vol. 93, Univelt Inc., San Diego, California, USA, 1996, pp. 201-220.
23. Wilson, A., (ed.), Jane's Space Directory 1993-94, 9th edition, United Kingdom, 1993.